

# Achieving the Heisenberg limit with Dicke States in noisy quantum metrology

Zain H. Saleem<sup>1,\*</sup>, Michael Perlin<sup>2,†</sup>, Anil Shaji<sup>3,‡</sup> and Stephen K. Gray<sup>4,§</sup>

Mathematics and Computer Science Division, Argonne National Laboratory, 9700 S Cass Ave, Lemont IL 60439<sup>1</sup>  
Inflection, Chicago, Illinois, USA<sup>2</sup>

School of Physics, IISER Thiruvananthapuram, Kerala, India 695551<sup>3</sup> and  
Center for Nanoscale Materials, Argonne National Laboratory, Lemont, Illinois 60439, USA<sup>4</sup>

(Dated: September 25, 2023)

Going beyond the standard quantum limit in noisy quantum metrology is a very challenging task. Here we show how Dicke states can be used to surpass the standard quantum limit and achieve the Heisenberg limit in open quantum systems. The system we study has qubits symmetrically coupled to a resonator and our objective is to estimate the coupling between the qubits and the resonator. The time-dependent quantum Fisher information with respect to the coupling is studied for this open quantum system where the same decay rates are assumed on all qubits. We show that when the system is initialized to a Dicke state with an optimal excitation number one can go beyond the standard quantum limit and achieve the Heisenberg limit even for finite values of the decays on the qubit and the resonator. For comparison, we find that the highly entangled GHZ state performs quite poorly. Our results show that one must consider not only the degree of entanglement of an initial probe state, but its resilience to noise in order to achieve optimum sensing performance.

*Introduction.*— A quantum probe with  $N$  elementary sub-units is the focus of discussions on quantum limited single parameter estimation [1–4]. The probe is chosen such that the parameter to be estimated appears in its Hamiltonian. A suitable initial state of the probe evolves for a fixed time in a manner that depends on the parameter value. The value can be then inferred from a read-out of the final state of the probe. Quantum mechanics places a fundamental limit on measurement precision, called the Heisenberg limit (HL), which constrains how the precision of parameter estimation improves as the number of probe-units is increased. According to the HL, scaling of the precision with the number of elementary sub-units cannot scale better than  $1/N$ . For a noiseless system, HL scaling can be saturated using entangled states of the probe [5]. In practice, though, environmental decoherence typically degrades metrologically useful entanglement; instead of HL, precision scales like  $1/\sqrt{N}$ , called the standard quantum limit (SQL), which can be achieved by using the  $N$  elementary sub-units independently. To surpass the SQL various clever strategies have been devised, such as squeezing the vacuum [6], monitoring the environment during the measurements [7] and taking advantage of non-Markovian dynamics [8] of the probe.

The quantum Cramer-Rao bound [9] dictates that the precision in the measurement of a parameter in a quantum experiment is bounded by the inverse of the quantum Fisher information (QFI). The QFI is a time-dependent quantity, and in open quantum systems it tends to have a peak value in time. In [10] the time dependence of the QFI was studied and, as expected, in open quantum

systems the best precision in the estimate of a parameter can be achieved by performing measurements near the times when the QFI is the largest. In this Letter we introduce a strategy for surpassing the SQL in a noisy quantum system that relies on making use of this optimum time concept, coupled with the use of Dicke states [11, 12] with appropriately chosen excitation numbers as initial probe states.

We investigate a qubit-cavity model in contact with an environment where both the qubits and the cavity are allowed to decay under the influence of noise from the environment. The parameter that is estimated is the coupling constant of the qubits to the cavity. The qubits constitute the quantum probe and we focus on studying the scaling of the uncertainty in its estimate with the number of qubit,  $N$ , the number of qubits in quantum probe. We calculate the scaling of the maximum value of the QFI in time with  $N$  and see for what choices of the initial states and decay rates of the qubits and the resonator we are able to surpass the SQL. The Hamiltonian of our system is permutationally symmetric, and this symmetry allows us to use a basis that reduces the dimensions of our problem and thus allows us to study the problem for relatively large values of  $N$  which would otherwise be computationally intractable. Dicke states are examples of permutationally symmetric states and we will show that when the excitation number of the Dicke states is chosen appropriately and the measurements are performed in an optimal time region, we can surpass the standard quantum limit and achieve the Heisenberg limit even in the presence of dissipation. We attribute such results to a competition between degree of entanglement in the initially prepared probe state with its resilience to noise. The significance of our results and our main motivation lies in the fact that Dicke states with modest excitation numbers can be realised in the laboratory [13–23] and exploring the interplay between noise and metrological precision can be investigated experimentally. In addition there are multi-

\* zsaleem@anl.gov

† mika.perlin@gmail.com

‡ shaji@iisertvm.ac.in

§ gray@anl.gov

ple theoretical proposals for producing such states in the laboratory [24–35], giving further relevance to our work.

*Quantum Fisher information.*—Consider the problem of estimating a parameter  $\theta$  in a quantum experiment and denote the (unbiased) estimator of this parameter by  $\hat{\theta}$ . The parameter dependent evolution of the probe is given by  $H_{\text{probe}} = \theta h$ , where  $h$  is an operator on the probe state. The uncertainty in the estimate of the parameter,  $\delta\hat{\theta}^2$ , is upper-bounded by the quantum Cramér-Rao Bound [36],

$$\delta\hat{\theta}^2 \geq \frac{1}{MF} \quad (1)$$

where  $M$  stands for the total number of application of the quantum probe and  $F$  is the QFI, which quantifies the responsiveness of the quantum state of the probe to changes in the measured parameter  $\theta$ . The QFI of a mixed state  $\rho = \sum_a \lambda_a |\lambda_a\rangle\langle\lambda_a|$  with respect to the parameter  $\theta$  is [37]

$$F = \sum_{\{a,b|\lambda_a+\lambda_b\neq 0\}} \frac{2}{\lambda_a + \lambda_b} |\langle\lambda_a|\partial_\theta\rho|\lambda_b\rangle|^2, \quad (2)$$

For closed evolution of the probe, the QFI has a quadratic time dependence while for open evolution an optimal measurement time may be present that the parameter estimation protocol would take advantage of [10]. We study the scaling of the peak value of QFI under open evolution as  $N$  gets larger.

*Model system.*—The qubit-cavity model that we study here is described by the Hamiltonian ( $\hbar = 1$ )

$$H = \Delta S_z + \omega a^\dagger a + g(a^\dagger S_- + a S_+), \quad (3)$$

where  $S_z = \frac{1}{2} \sum_{i=1}^N \sigma_z^{(i)}$ , and  $S_\pm = \frac{1}{2} \sum_{i=1}^N \sigma_\pm^{(i)}$  are collective spin operators expressed in terms of the Pauli matrices,  $\sigma_x$ ,  $\sigma_y$  and  $\sigma_z$  with  $\sigma_\pm = \sigma_x \pm i\sigma_y$ ;  $a^\dagger, a$  are bosonic raising and lowering operators for the cavity;  $\Delta$  is the qubit excitation energy;  $\omega$  is the resonator frequency; and  $g$  is the qubit-cavity coupling strength. Our focus will be on the QFI with respect to measurement of the coupling constant,  $g$ , i.e.,  $\theta = g$  in Eq. (2). Since we are only concerned with estimating the coupling we work in the interaction picture and focus on  $H_{\text{probe}} = g(a^\dagger S_- + a S_+)$  or equivalently setting  $\omega = \Delta = 0$ . The state of the quantum probe undergoes open evolution described by the Gorini-Kossowski-Sudarshan-Lindblad (GKSL) equation [38–41],

$$\dot{\rho} = -i[H, \rho] + \sum_{j=q,r} \Gamma_j \left[ L_j \rho L_j^\dagger - \frac{1}{2} \{L_j^\dagger L_j, \rho\} \right]. \quad (4)$$

where the Lindblad jump operators  $L_j$  corresponding to qubit ( $q$ ) and the resonator ( $r$ ) decay are respectively  $L_q = S_-$  and  $L_r = a$ , with associated decay rates  $(\Gamma_q, \Gamma_r) = (\gamma, \kappa)$ .

In principle, if the cavity excitation number is bounded above by the qubit number  $N$ , the Hilbert space of the

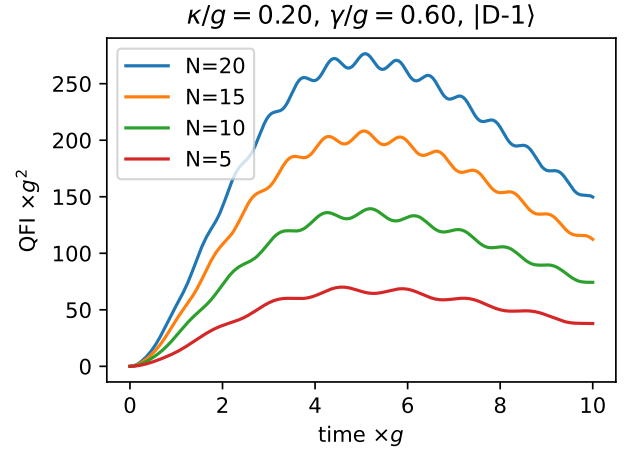


FIG. 1. Time-dependent QFI for different qubit numbers,  $N$ , for an initial Dicke-1 state with relatively small qubit ( $\gamma$ ) and resonator ( $\kappa$ ) decay rates. The peak structures increase with  $N$  for this case.

combined qubit-cavity system has dimension  $(N+1)2^N$ . Operators on this Hilbert space (such as  $\rho$ ), in turn, have  $O(N^2 4^N)$  degrees of freedom, which severely limits computational capability even for moderately large  $N$ . However, the spin-permutational symmetry of the Hamiltonian allows us to perform calculations in a symmetric basis that grows more modestly as  $O(N^5)$  [12, 42]. Specifically, we can expand any operator on the qubit-cavity Hilbert space in a basis of matrix elements of the form  $|Jn\rangle\langle Jm| \otimes |\ell\rangle\langle k|$ , where  $J \in \{\frac{N}{2}, \frac{N}{2} - 1, \dots\}$  is a positive total spin length,  $n, m \in \{J, J-1, \dots, -J\}$  are spin projections onto the spin quantization axis, and  $\ell, k \in \{0, 1, \dots, N\}$  are cavity occupation numbers.

Our main focus is on the case where the quantum probe initialised in Dicke states of the qubits with resonator in its ground state,

$$|\text{D-}n\rangle = |\phi_n\rangle \otimes |0\rangle, \quad |\phi_n\rangle \propto S_+^n |0\rangle^{\otimes N}, \quad (5)$$

where  $S_+^n$  generates a sum of all permutations of  $|0\rangle^{\otimes(N-n)} |1\rangle^{\otimes n}$ . Here  $|\phi_n\rangle$  is a normalized Dicke state of  $N$  qubits, which can be equivalently defined as a uniform superposition of all  $N$ -qubit states with exactly  $n$  excitations, e.g.,

$$|\phi_1\rangle = \frac{1}{\sqrt{N}} (|100\dots\rangle + |010\dots\rangle + |001\dots\rangle). \quad (6)$$

$|\phi_1\rangle$  is also known as the  $N$ -qubit W state [43]. For ease of language, we generally refer to  $|\text{D-}n\rangle$  as the Dicke- $n$  state of the qubit-resonator system. For comparison with the  $|\text{D-}n\rangle$  state we also consider the  $X$ -polarized state

$$|\text{X}\rangle = \frac{1}{\sqrt{2^N}} (|0\rangle + |1\rangle)^{\otimes N} \otimes |0\rangle, \quad (7)$$

and the GHZ state [44]

$$|\text{GHZ}\rangle = \frac{1}{\sqrt{2}} (|0\rangle^{\otimes N} + |1\rangle^{\otimes N}) \otimes |0\rangle, \quad (8)$$

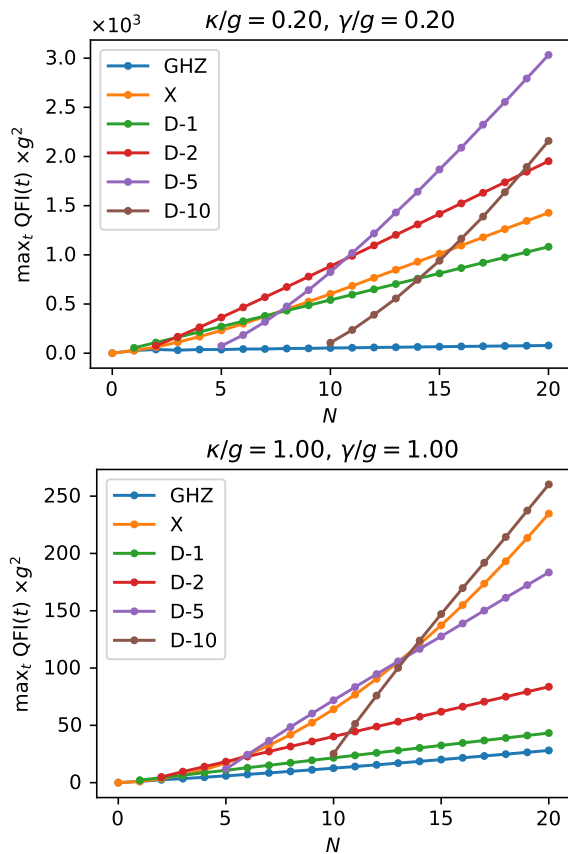


FIG. 2. Scaling of the maximum QFI with respect to time for fixed qubit and resonator decay rates, and different initial states. The upper and lower panels correspond to small and large values of the decay rates, respectively.

which are again defined with the resonator in its ground state.

*Time-dependence of the QFI for  $N$  qubits.*—In Fig. 1 we show a plot of the time-dependent QFI for the Dicke-1 initial state for different values of  $N$ , keeping the decay constants on all the qubits and the resonators fixed. One sees that on average the QFI rises and then falls in time, with some oscillatory substructure superimposed. The region of largest QFI values and also the associated overall maximum QFI value increase in magnitude with increasing  $N$ . This behavior is not limited to the Dicke-1 state and happens for all the other Dicke- $n$  states and for the GHZ and  $X$ -polarized initial states as well. In Fig. 2 we provide plots of how the maximum QFI value scales with  $N$ . Note that we use  $N$  to quantify the resources that go into the measurement of  $g$  even though, strictly speaking, we have  $N$  qubits plus a resonator whose Hilbert space dimension grows as  $N + 1$ . It is interesting to note in Fig. 2 that the GHZ state, despite being maximally entangled by some measures, scales very poorly for both small and large values of decay rates. This is due to the fragility of the GHZ state to decoherence. For example, measuring just one qubit

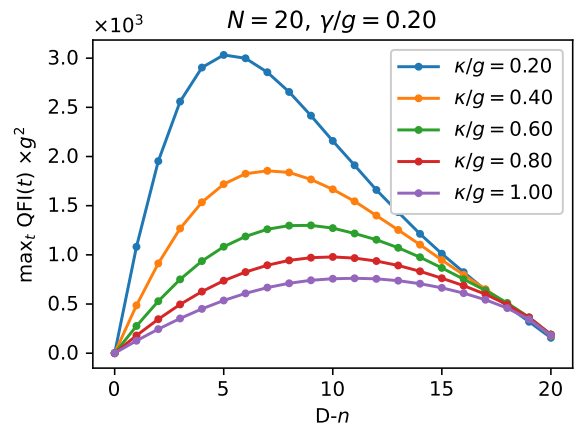


FIG. 3. Variation of the maximum QFI (with respect to time) with Dicke excitation number for  $N = 20$  qubits and varying resonator decay rate,  $\kappa$ , for fixed qubit decay rate,  $\gamma$ .

collapses the GHZ state into a separable state, whereas this is not the case for the W state or, indeed, most of the Dicke states. For large values of the decay constants (lower panel of Fig. 2) the initially unentangled  $X$ -state scales in a manner almost comparable to the large excitation Dicke states which is due to the dissipation-induced entanglement [45] occurring because of the coupling between the qubits and the resonator. We note, however, that the  $X$ -state is only competitive with the best Dicke states in the limit of relatively high dissipation and low QFI magnitudes, i.e. in a limit less well suited to achieving high-precision sensing.

*Optimal excitation number of Dicke states.*—Figure 2 shows that, depending on the number of qubits,  $N$ , there can be optimal Dicke state excitation numbers. In the case of low dissipation (upper panel of Fig. 2) for example, Dicke-2 has the larger QFI for  $N = 5-10$ , whereas Dicke-5 has the higher QFI for  $N > 10$ . In Fig. 3 we plot the maximum value of the QFI against different Dicke excitation numbers for  $N = 20$  and see that there is indeed an optimal value of the excitation number for which the maximum value of the QFI is the largest for each  $\kappa$  considered. By the geometric entanglement measure, for fixed  $N$ , it turns out that the most entangled Dicke state is equal to or close to Dicke- $N/2$  [46]. For the  $N = 20$  case of Fig. 3, this would correspond to Dicke-10. The results of Fig. 3, however, show optimum Dicke states ranging from Dicke-5 at the lowest  $\kappa$  considered to Dicke-11 at the highest  $\kappa$  considered, again consistent with entanglement alone not being the best gauge of sensing quality and that a competition between degree of entanglement and resilience to noise leads to the optimum initial probe state.

Finally, we consider if certain ranges of the decay constants associated with the qubits and the resonator can lead to scaling that surpasses the standard quantum limit or SQL. To accomplish this, we fit  $y(N) = aN^b + c$  to the maximum QFI vs  $N$  plots for a large range of decay

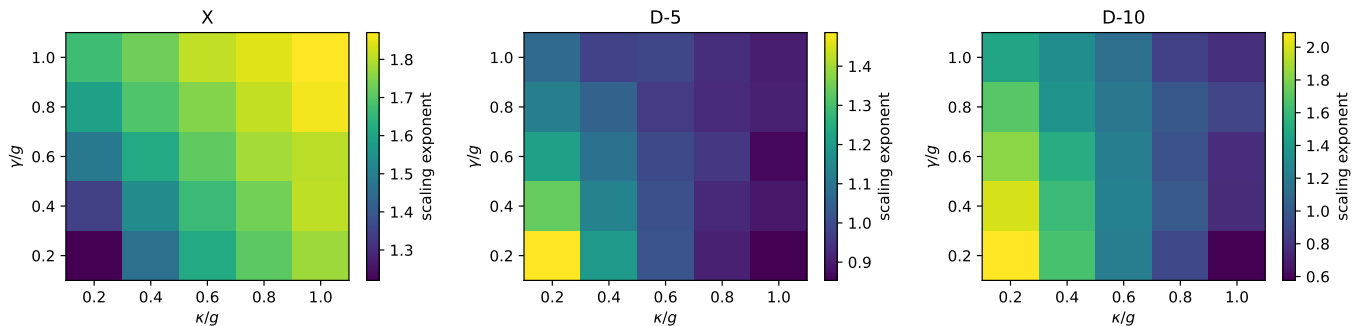


FIG. 4. The scaling exponent  $b$  obtained by fitting the time-maximized QFI to the qubit number  $N$  as  $\text{QFI}(N) = aN^b + c$  for different resonator and qubit decay rates  $\kappa$  and  $\gamma$  and three initial states.

constant values and extract the scaling exponent,  $b$ . The results of our numerical simulations are summarized in Fig. 4 where we plot the exponent  $b$  for different values of the decay constants for three different initial states, the  $X$ -state, Dicke-5 state and Dicke-10 state. In these plots  $b = 1$  corresponds to the SQL and  $b = 2$  corresponds to the Heisenberg limit. Regarding the initially unentangled  $X$ -state, scaling closer to the SQL limit occurs for low decay constant values, as might be expected. A transition to much better than SQL scaling occurs as higher decay constants are considered due to dissipation-induced entanglement but, as previously noted, the actual magnitudes of the QFI can be orders of magnitude smaller than what is achievable with Dicke states. For the Dicke states, it can be clearly seen that for certain, low but finite values of the decay rates the Dicke states are able to go above the SQL and even achieve the Heisenberg limit.

*Conclusions and future directions.*—We studied the quantum Fisher information associated with inferring a parameter in an open quantum system corresponding to  $N$  qubits coupled to a resonator. We used the permutational symmetry to restrict the dimension of the density matrix allowing us to explore up to  $N = 20$  qubits. Our investigation shows that for a fixed number of qubits, there is an optimal value of the excitation number of the initial Dicke state which is the most resilient to noise effects and initializing the sensor in this state can help us achieve the Heisenberg limit. The versatility, resilience

to noise and experimental accessibility of Dicke states can be leveraged to design optimal quantum metrology schemes in the presence of noise for other parameters. The detuning  $\Delta$  from Eq. (3) is one such candidate parameter, as well as the decay parameters  $\kappa$  and  $\gamma$ .

A general concept that has emerged from our work is that there is a trade off between degree of entanglement and resilience to noise, with some highly entangled states such as the GHZ state performing quite poorly due to a lack of resilience to noise. The ability to produce Dicke states in the laboratory [13–23] offers the prospect of studying this trade off experimentally based on our numerical results.

*Acknowledgments.*—This material is based upon work supported by the U.S. Department of Energy Office of Science National Quantum Information Science Research Centers. S.K.G. and Z.H.S. were supported by the Q-NEXT Center. Work performed at the Center for Nanoscale Materials, a U.S. Department of Energy Office of Science User Facility, was supported by the U.S. DOE Office of Basic Energy Sciences, under Contract No. DE-AC02-06CH11357. A. S. was supported by QuEST grant No Q-113 of the Department of Science and Technology, Government of India. The results in this work were obtained from simulations using  $\sim 1000$  CPU-hours on the Bebop computing cluster at Argonne National Laboratory.

- 
- [1] V. Giovannetti, S. Lloyd, and L. Maccone, Advances in quantum metrology, *Nature Photonics* **5**, 222 (2011).
  - [2] G. Tóth and I. Apellaniz, Quantum metrology from a quantum information science perspective, *Journal of Physics A: Mathematical and Theoretical* **47**, 424006 (2014).
  - [3] W. Nawrocki, *Introduction to quantum metrology*, 2nd ed. (Springer Nature Switzerland, Cham, Switzerland, 2019).
  - [4] E. Polino, M. Valeri, N. Spagnolo, and F. Sciarrino, Photonic quantum metrology, *AVS Quantum Science* **2**, 024703 (2020).
  - [5] V. Giovannetti, S. Lloyd, and L. Maccone, Quantum-enhanced measurements: beating the standard quantum limit, *Science* **306**, 1330 (2004).
  - [6] L. Pezzé and A. Smerzi, Mach-Zehnder interferometry at the heisenberg limit with coherent and squeezed-vacuum light, *Physical Review Letters* **100**, 073601 (2008).
  - [7] M. B. Plenio and S. F. Huelga, Sensing in the presence of an observed environment, *Physical Review A* **93**, 032123 (2016).
  - [8] A. W. Chin, S. F. Huelga, and M. B. Plenio, Quantum metrology in non-Markovian environments, *Physical Review Letters* **109**, 233601 (2012).
  - [9] H. Cramér, A contribution to the theory of statisti-

- cal estimation, *Scandinavian Actuarial Journal* **1946**, 85 (1946).
- [10] Z. H. Saleem, A. Shaji, and S. K. Gray, Optimal time for sensing in open quantum systems, *Physical Review A* **108**, 022413 (2023).
- [11] R. H. Dicke, Coherence in spontaneous radiation processes, *Physical Review* **93**, 99 (1954).
- [12] N. Shammah, S. Ahmed, N. Lambert, S. De Liberato, and F. Nori, Open quantum systems with local and collective incoherent processes: Efficient numerical simulations using permutational invariance, *Physical Review A* **98**, 063815 (2018).
- [13] Y.-Q. Zou, L.-N. Wu, Q. Liu, X.-Y. Luo, S.-F. Guo, J.-H. Cao, M. K. Tey, and L. You, Beating the classical precision limit with spin-1 Dicke states of more than 10,000 atoms, *Proceedings of the National Academy of Sciences* **115**, 6381 (2018).
- [14] L. Chen, L. Lu, L. Xia, Y. Lu, S. Zhu, and X.-s. Ma, On-Chip Generation and Collectively Coherent Control of the Superposition of the Whole Family of Dicke States, *Physical Review Letters* **130**, 223601 (2023).
- [15] A. Chiuri, G. Vallone, N. Bruno, C. Macchiavello, D. Bruß, and P. Mataloni, Hyperentangled Mixed Phased Dicke States: Optical Design and Detection, *Physical Review Letters* **105**, 250501 (2010).
- [16] F. Haas, J. Volz, R. Gehr, J. Reichel, and J. Estève, Entangled States of More Than 40 Atoms in an Optical Fiber Cavity, *Science* **344**, 180 (2014).
- [17] H. Häffner, W. Hänsel, C. F. Roos, J. Benhelm, D. Chekhal kar, M. Chwalla, T. Körber, U. D. Rapol, M. Riebe, P. O. Schmidt, C. Becher, O. Gühne, W. Dür, and R. Blatt, Scalable multiparticle entanglement of trapped ions, *Nature* **438**, 643 (2005).
- [18] D. B. Hume, C. W. Chou, T. Rosenband, and D. J. Wineland, Preparation of Dicke states in an ion chain, *Physical Review A* **80**, 052302 (2009).
- [19] A. Noguchi, K. Toyoda, and S. Urabe, Generation of Dicke States with Phonon-Mediated Multilevel Stimulated Raman Adiabatic Passage, *Physical Review Letters* **109**, 260502 (2012).
- [20] R. Prevedel, G. Cronenberg, M. S. Tame, M. Paternostro, P. Walther, M. S. Kim, and A. Zeilinger, Experimental Realization of Dicke States of up to Six Qubits for Multiparty Quantum Networking, *Physical Review Letters* **103**, 020503 (2009).
- [21] K. Toyoda, T. Watanabe, T. Kimura, S. Nomura, S. Haze, and S. Urabe, Generation of Dicke states using adiabatic passage, *Physical Review A* **83**, 022315 (2011).
- [22] W. Wieczorek, R. Krischek, N. Kiesel, P. Michelberger, G. Tóth, and H. Weinfurter, Experimental Entanglement of a Six-Photon Symmetric Dicke State, *Physical Review Letters* **103**, 020504 (2009).
- [23] S. Yu, M. Titze, Y. Zhu, X. Liu, and H. Li, Observation of scalable and deterministic multi-atom Dicke states in an atomic vapor, *Optics Letters* **44**, 2795 (2019).
- [24] S. Aktar, A. Bärtschi, A.-H. A. Badawy, and S. Eidenbenz, A Divide-and-Conquer Approach to Dicke State Preparation, *IEEE Transactions on Quantum Engineering* **3**, 1 (2022).
- [25] K. Chakraborty, B.-S. Choi, A. Maitra, and S. Maitra, Efficient quantum algorithms to construct arbitrary Dicke states, *Quantum Information Processing* **13**, 2049 (2014).
- [26] S. S. Ivanov, N. V. Vitanov, and N. V. Korolkova, Creation of arbitrary Dicke and NOON states of trapped-ion qubits by global addressing with composite pulses, *New Journal of Physics* **15**, 023039 (2013).
- [27] S. Kasture, Scalable approach to generation of large symmetric Dicke states, *Physical Review A* **97**, 043862 (2018).
- [28] L. Lamata, C. E. López, B. P. Lanyon, T. Bastin, J. C. Retamal, and E. Solano, Deterministic generation of arbitrary symmetric states and entanglement classes, *Physical Review A* **87**, 032325 (2013).
- [29] F. Mu, Y. Gao, H. Yin, and G. Wang, Dicke state generation via selective interactions in a Dicke-Stark model, *Optics Express* **28**, 39574 (2020).
- [30] S. Raghavan, H. Pu, P. Meystre, and N. P. Bigelow, Generation of arbitrary Dicke states in spinor Bose–Einstein condensates, *Optics Communications* **188**, 149 (2001).
- [31] V. M. Stojanović and J. K. Nauth, Dicke-state preparation through global transverse control of Ising-coupled qubits, *Physical Review A* **108**, 012608 (2023).
- [32] Y. Wang and B. M. Terhal, Preparing Dicke states in a spin ensemble using phase estimation, *Physical Review A* **104**, 032407 (2021).
- [33] J.-H. Wei, B. Qi, H.-Y. Dai, J.-H. Huang, and M. Zhang, Deterministic generation of symmetric multi-qubit Dicke states: an application of quantum feedback control, *IET Control Theory & Applications* **9**, 2500 (2015).
- [34] C. Wu, C. Guo, Y. Wang, G. Wang, X.-L. Feng, and J.-L. Chen, Generation of Dicke states in the ultrastrong-coupling regime of circuit QED systems, *Physical Review A* **95**, 013845 (2017).
- [35] C. Zhao and L. Ye, Efficient scheme for the preparation of symmetric Dicke states via cross-Kerr nonlinearity, *Physics Letters A* **375**, 401 (2011).
- [36] A. S. Holevo, *Probabilistic and statistical aspects of quantum theory*, Vol. 1 (Springer Science & Business Media, 2011).
- [37] J. Liu, H. Yuan, X.-M. Lu, and X. Wang, Quantum Fisher information matrix and multiparameter estimation, *Journal of Physics A: Mathematical and Theoretical* **53**, 023001 (2019).
- [38] V. Gorini, A. Kossakowski, and E. C. G. Sudarshan, Completely positive dynamical semigroups of N-level systems, *Journal of Mathematical Physics* **17**, 821 (1976), publisher: American Institute of Physics.
- [39] G. Lindblad, On the generators of quantum dynamical semigroups, *Communications in Mathematical Physics* **48**, 119 (1976).
- [40] D. Chruściński and S. Pascazio, A Brief History of the GKLS Equation, *Open Systems & Information Dynamics* **24**, 1740001 (2017).
- [41] D. Manzano, A short introduction to the Lindblad master equation, *Aip Advances* **10**, 025106 (2020).
- [42] B. A. Chase and J. Geremia, Collective processes of an ensemble of spin-1/2 particles, *Physical Review A* **78**, 052101 (2008).
- [43] W. Dür, G. Vidal, and J. Cirac, Three qubits can be entangled in two inequivalent ways, *Physical Review A* **62**, 062314 (2000).
- [44] D. M. Greenberger, M. A. Horne, and A. Zeilinger, Going beyond Bell’s theorem, in *Bell’s Theorem, Quantum Theory and Conceptions of the Universe*, edited by M. Kafatos (Springer Netherlands, Dordrecht, 1989) pp. 69–72.
- [45] F. Benatti, R. Floreanini, and M. Piani, Environment in-

duced entanglement in Markovian dissipative dynamics, Physical Review Letters **91**, 070402 (2003).

- [46] J. Martin, O. Giraud, P. Braun, and T. Bastin, Multiqubit symmetric states with high geometric entanglement, Physical Review A **81**, 062347 (2010).

The submitted manuscript has been created by UChicago Argonne, LLC, Operator of Argonne National Laboratory (“Argonne”). Argonne, a U.S. Department of Energy Office of Science laboratory, is operated under Contract No. DE-AC02-06CH11357. The U.S. Gov-

ernment retains for itself, and others acting on its behalf, a paid-up nonexclusive, irrevocable worldwide license in said article to reproduce, prepare derivative works, distribute copies to the public, and perform publicly and display publicly, by or on behalf of the Government. The Department of Energy will provide public access to these results of federally sponsored research in accordance with the DOE Public Access Plan (<http://energy.gov/downloads/doe-public-access-plan>).